

The Michelucci Tower in Livorno, Italy

*Original*

The Michelucci Tower in Livorno, Italy / Carpinteri, A., Lacidogna, G., Mamone, A.. - In: PROCEEDINGS OF THE INSTITUTION OF CIVIL ENGINEERS. CIVIL ENGINEERING. - ISSN 0965-089X. - STAMPA. - 179:1(2026), pp. 68-83. [10.1680/jcien.25.00196]

*Availability:*

This version is available at: 11583/3007607 since: 2026-02-14T18:40:12Z

*Publisher:*

Emerald Publishing

*Published*

DOI:10.1680/jcien.25.00196

*Terms of use:*

This article is made available under terms and conditions as specified in the corresponding bibliographic description in the repository

*Publisher copyright*

Elsevier postprint/Author's Accepted Manuscript

© 2026. This manuscript version is made available under the CC-BY-NC-ND 4.0 license  
<http://creativecommons.org/licenses/by-nc-nd/4.0/>. The final authenticated version is available online at:  
<http://dx.doi.org/10.1680/jcien.25.00196>

(Article begins on next page)

# The Michelucci Tower in Livorno (Italy)

Alberto Carpinteri<sup>1</sup>, Giuseppe Lacidogna<sup>2\*</sup>, Andrea Mamone<sup>2</sup>

<sup>1</sup> Professor, Department of Civil Engineering and Intelligent Construction, Shantou University, Shantou, China

<sup>2</sup> Professor, Department of Structural, Geotechnical and Building Engineering, Politecnico di Torino, Turin, Italy.

<sup>2</sup> Engineer, Department of Structural, Geotechnical and Building Engineering, Politecnico di Torino, Turin, Italy.

\*Corresponding author: giuseppe.lacidogna@polito.it (G. Lacidogna);

**Abstract:** In the contemporary era, civil engineering design is predominantly carried out using software tools that have significantly reduced operational time by automatic calculations. However, these tools often require a substantial amount of data input and extensive post-processing of results. In the context of high-rise buildings, the General Algorithm (GA) and its software implementation represent a promising solution to this challenge, ensuring a significant improvement in efficiency during both data input and result analysis. The TaBu (Tall Building Structural System) computational code, which implements the analytical model within the Matlab environment, despite inherent modeling limitations, has demonstrated in several previous studies its ability to estimate results comparable to those obtained through FEM analysis, and deviations often less than 10%. However, in cases involving complex geometries like the Michelucci Tower in Livorno (Italy), the differences can reach approximately 20-30%, due to the simplifications inherent in the analytical approach.

Nevertheless, it can be considered a valuable tool for preliminary building analyses, facilitating the subsequent transition to more detailed modeling. This study is aimed at comparing the estimated horizontal displacements of a high-rise building, the so-called Michelucci Tower, using the TaBu software (derived from an analytical model) and the FEM software DOLMEN (developed by CDM DOLMEN).

**Keywords:** Michelucci Tower; High-Rise Building Analysis; Civil Engineering Software; Structural Modeling; Displacement Estimation; Efficiency in Design Processes

## 1. Introduction

The twentieth century witnessed significant innovations in civil engineering constructions, marked by the emergence of novel structural solutions, including high-rise buildings. The Livorno Tower, in particular, features an unconventional volumetric configuration that distinguishes it from contemporary structures.

Designed by Giovanni Michelucci, a renowned Italian architect of the 20th century, the skyscraper was constructed between 1961 and 1966. Standing approximately 90 meters tall, it comprises 26 stories above ground, culminating in a terrace at its highest level. At the time of its completion, it was among the tallest structures in Italy (Fig. 1).

The architectural composition of the building is characterized by two distinct structural parts: a polygonal base plate, which encompasses the first six stories and serves as a pedestal, and a tower that rises above it. The tower is further subdivided into five sections, with façades aligned with those of the base plate.

Notably, the tower exhibits remarkable originality in its design, adhering to an entirely innovative and, at times, seemingly chaotic scheme. This is evidenced by a series of additions and subtractions dictated by the presence of projections and bow windows (protruding structures akin to enclosed balconies), which contribute to the building's distinctive architectural identity.

Such complex and unconventional architectural features often pose significant challenges for structural analysis and assessment. Therefore, understanding and accurately predicting the building's response to environmental loads becomes crucial for ensuring safety and performance.

The main contribution of this paper lies in demonstrating the effectiveness of a simplified, analytical modeling approach (using the TaBu software based on the General Algorithm) for estimating

horizontal displacements in high-rise buildings, validated through comparison with detailed FEM results. By applying this approach to a structure characterized by intricate and seemingly chaotic design, as the Livorno Tower, the study highlights the potential of simplified models to provide reliable initial insights. The study provides new insights into the accuracy (in this case the maximum deviations range within 20-30%) of this rapid assessment method for wind and seismic loads, emphasizing its significant time-saving advantages. It underscores that, despite the complexity and uniqueness of such architectural schemes, simplified analytical tools can serve as practical and efficient means for early-stage structural evaluation, facilitating informed decision-making also when detailed data is limited. The findings support the practical application of analytical tools in preliminary structural analyses, offering a balance between computational efficiency and result accuracy.

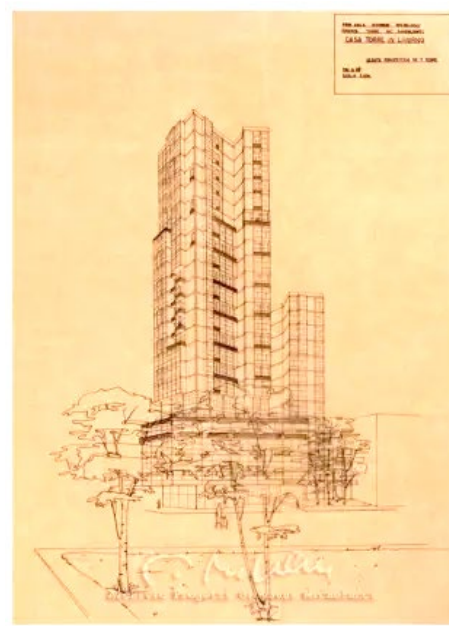


Fig. 1. View of the tower and perspective view taken from the on-line documents of the Giovanni Michelucci Foundation (Thanks to the Giovanni Michelucci Foundation for permission to use the archive sources of the "Grattacielo Roma, Livorno 1956-1966", <http://db.michelucci.it/archivi/progetti/?opera=P125>).

## 2. Preliminary investigations

In consideration of the temporal context of the construction, it was immediately apparent that it was not possible to easily find the entire executive design documentation.

For structures made of plain or reinforced concrete, Article 4 of Royal Decree No. 2229 of November 16, 1939, required private entities to file a notice of works with the Prefecture of the relevant province, accompanied by a preliminary design, before commencing construction. The same article mandated the submission of a Final Acceptance Certificate to the Prefecture upon completion of the works (see Fig. 2). However, while the design documentation, including all executive details, had to be kept on-site and made available for potential inspections, there was no legal obligation to submit a copy for official record-keeping. In contrast, structures built on behalf of the State and under the supervision of state technical authorities were exempt from the requirement to file a notice with the Prefecture.

**Art. 4.**

Ai costruttori, prima di iniziare la costruzione delle opere, di cui all'art. 1, è fatto obbligo di presentarne alla prefettura della provincia denuncia, corredata di una copia del progetto di massima.

Nei cantieri, dal giorno dell'inizio a quello di ultimazione dei lavori, deve essere conservata una copia dei particolari esecutivi di tutte le parti delle opere in costruzione, datati e firmati dal progettista, dal direttore dei lavori e dal costruttore. Il direttore dei lavori deve riportare nei disegni, con inchiostro di colore diverso, tutte le modifiche introdotte nelle opere all'atto esecutivo, datandole e firmandole.

...

Al termine dei lavori il committente, per ottenere la licenza di uso della costruzione, deve presentare alla prefettura il certificato di collaudo delle opere, rilasciato da un ingegnere di riconosciuta competenza, iscritto all'albo.

(a)

**Article 4.**

Prior to commencing the construction of the works referred to in Article 1, builders are required to submit a notification to the prefecture of the province, accompanied by a copy of the preliminary project.

At construction sites, from the start date until the completion of the works, a copy of the detailed execution plans for all parts of the works under construction must be kept, dated and signed by the designer, the site manager, and the builder. The site manager must record in the drawings, using ink of a different color, all modifications made during the execution phase, dating and signing them.

...

Upon completion of the works, the client, in order to obtain the occupancy permit, must present to the prefecture the testing certificate of the works, issued by a recognized and registered engineer with proven competence.

(b)

Fig. 2. Excerpt from Royal Decree No. 2229 of November 16, 1939, "Regulations for the Execution of Structures in Plain or Reinforced Concrete". (a) Original version in Italian. (b) English translation.

As a result, a comprehensive and meticulous document investigation was necessary for the authors of the present paper. An initial search at the Giovanni Michelucci Foundation in Fiesole (Florenz) led to the discovery of 17 drawings, including various elevations and several floor plans (Fig. 3). However, subsequent investigations conducted at the Civil Engineering Department, the Municipality of Livorno, and the building administrator were less successful, yielding no additional design documentation.

Given the historical and architectural significance of the tower, an extensive bibliographic investigation was undertaken. This research identified specialized texts containing further detailed floor plans for several key levels of the building, including (Luseroni, 2010; Fabbrizi, 2016).

Although these documents primarily focus on the architectural aspects of the building, they provide a reasonably accurate representation of the main geometric characteristics of the typical floors.

At present, no structural documentation has been found.

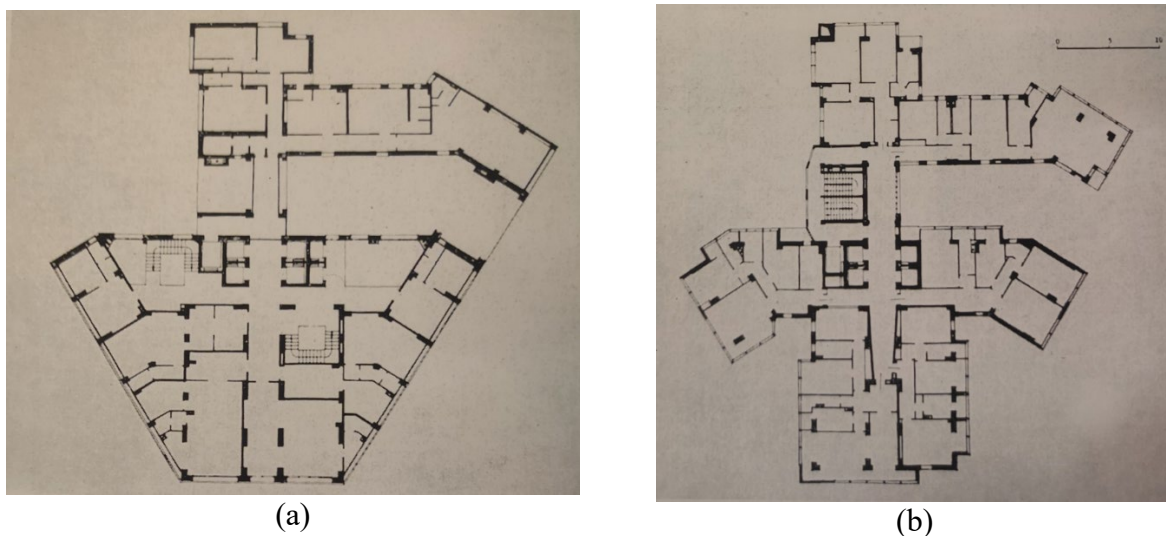


Fig. 3. First Floor Plan (left) and Floor Plan for Levels 8 to 11 (right). Extracted from the online documents of the Giovanni Michelucci Foundation (<http://db.michelucci.it/archivi/progetti/?opera=P125>).

### 3. Structural features and construction phase challenges

The first challenges in erecting the structure emerged during the foundation works. The soil conditions in the city of Livorno are characterized by high clay contents and significant moisture levels, necessitating extensive and complex preparatory measures. The foundation system required

the construction of a sheet pile, essentially a large metal caisson filled with tons of concrete and reinforced with 500 tons of steel. Additionally, 600 piles, each with a diameter of 40 cm and a length of 20 meters, were driven into the ground. These measures resulted in the formation of a stable platform capable of supporting the entire structural complex.

Once the foundations were completed, construction progressed at a remarkable pace: by September 1963, the thirteenth floor had already been reached, and by April 1964, the twenty-seventh floor was completed. By late summer of the same year, finishing works commenced, requiring meticulous attention due to the integration of specific decorative and aesthetic elements. However, in the early months of 1965, construction of the tower came to an end. Workers were progressively laid off, and by February of that year, only two remained on-site.

According to Fillea-CGIL, the Italian trade union representing workers in the construction, and part of the larger CGIL (Italian General Confederation of Labour), the province of Livorno, like the rest of the country, was experiencing a severe crisis in the construction sector. Consequently, numerous construction sites either reduced their activities or limited working hours. Conversely, the construction company attributed the delay to seasonal factors, arguing that the freezing temperatures of January and February rendered construction at considerable heights unfeasible. Due to these adverse weather conditions, work resumed only in April 1965. By May, construction activities were underway on both the façade and the interior, including the installation of hydraulic and electrical systems.

By the end of 1966, following a construction period spanning a decade, the building designed by Michelucci was finally completed.

### **3.1 Volumetric and structural description**

The arrangement of structural elements within the building exhibits considerable variability across different floors.

The ground floor presents the most distinct configuration compared to the upper levels. At this level, the structure is divided into two separate blocks by a vehicular passage that connects the two streets

flanking the building. Access to the upper floors is provided by two staircases and seven elevators; however, the staircases extend only up to the sixth floor.

Most columns are integrated within the cladding or infill walls, thereby minimizing their visual and spatial impact. In contrast, the shear walls follow a non-symmetrical configuration, except for those enclosing the elevator shafts (Fig. 4).

The horizontal slabs are supported by load-bearing dropped beams, which reveal their structural layout as well as the orthogonal orientation of the secondary joists.

From the third floor onwards, cantilevered perimeter structures emerge, extending up to the sixth floor. Beyond this level, the seventh floor primarily serves as a roof for the underlying block. In this configuration, the external projections transform into open-air spaces, leading to a significant structural variation due to the absence of two large sections of the structure.

A notable structural change occurs on the fifteenth floor, where the right rear wing of the building is entirely removed (Fig. 5).

With regard to shear walls, it is important to note that those associated to the first two elevator shafts are interrupted, as these elevators only serve the floors below the seventh level.

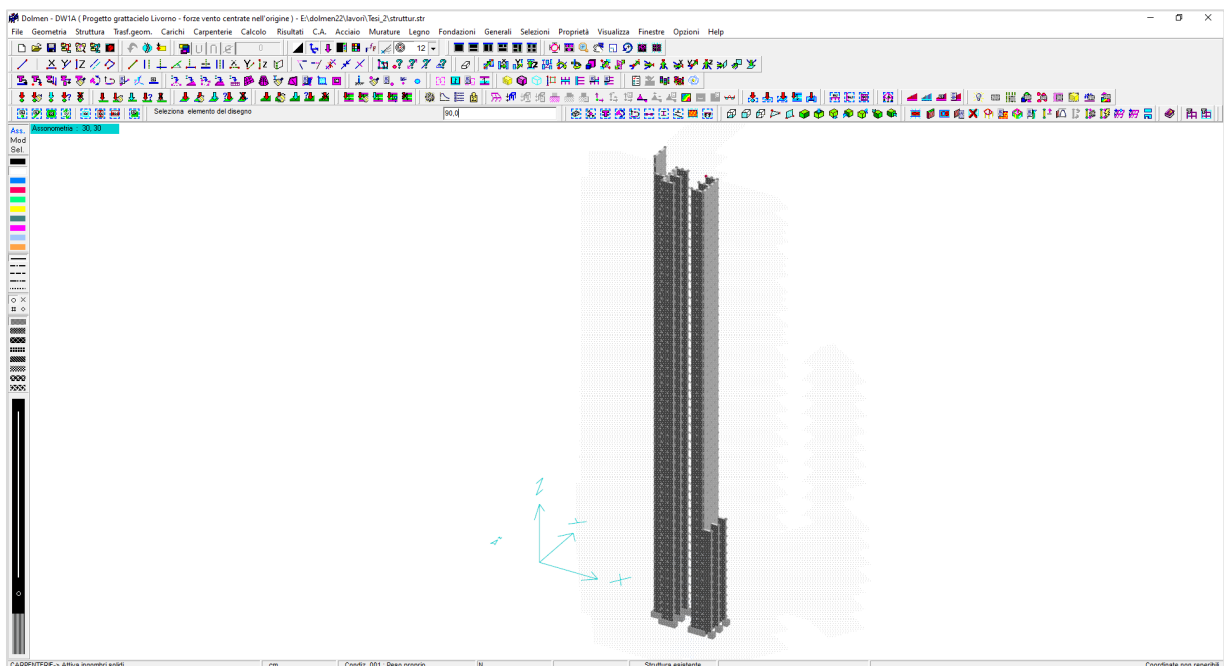


Fig. 4. 3D FEM Model: View of the central reinforced concrete shear walls.

The final identifiable structural block comprises the floors between the 16th and 26th levels. The primary structural modifications compared to the preceding block include the removal of the emergency elevator and the two elevators that previously served floors 7 through 15. Despite these changes, the overall floor layouts remain largely consistent, with only minor geometric variations in the balcony configurations and the introduction of additional architectural details, such as the two ramps of the emergency staircase.

The top floor consists of an accessible roof, featuring open-air peripheral areas and a central volume resembling an attic space with a roof covering. The emergency staircase, which serves as the sole access to this level, leads directly into this box-shaped structure, which is equipped with exits providing direct access to the terrace.

In conclusion, five distinct typical floor configurations were identified with reasonable accuracy, allowing for a comprehensive definition of the volumetric composition of the tower (Fig. 5).

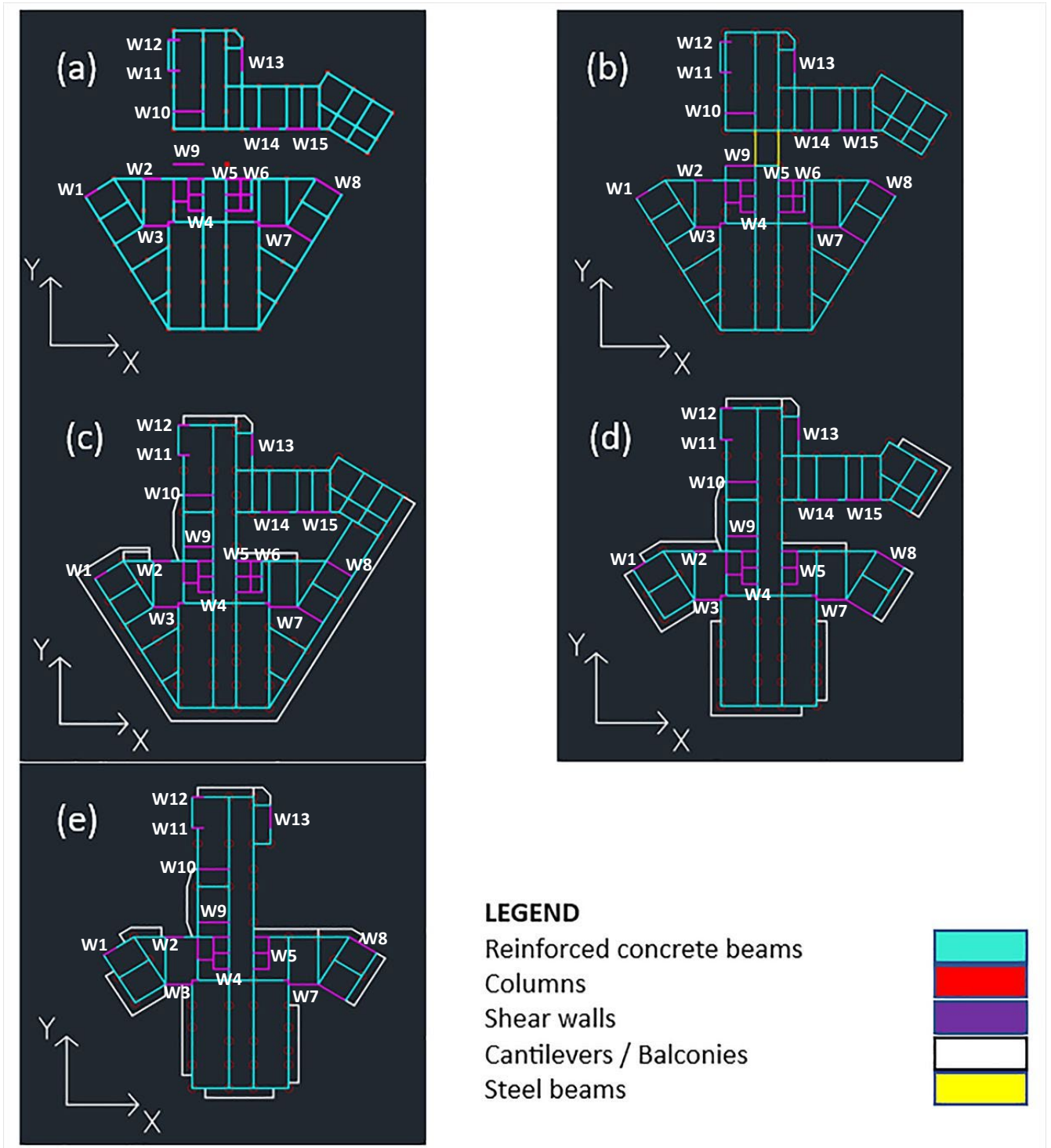


Fig. 5. Five distinct typical floor plans of the Livorno skyscraper, illustrating the lateral load resisting systems and their continuity across different levels. The plans include wall numbering (W1, W2, etc.) to facilitate tracking of the structural elements. (a) Ground floor; (b) First floor; (c) Floors 2 to 6; (d) Floors 7 to 15; (e) Floors 16 to 26.

### **3.2 Construction details**

Due to the absence of structural documentation and considering the objectives of this study, the structural elements were defined through a meticulous analysis of the available architectural drawings and reasonable design assumptions.

Since the primary goal was to evaluate the feasibility of a simplified modeling approach for estimating horizontal displacements, significant effort was made to accurately identify and approximate the dimensions of the structural elements.

The investigations clearly established the positions of the main structural components and the spans of the load-bearing beams. However, detailed data regarding the exact thickness of the shear walls and the precise dimensions of beam and column sections were unavailable. Where necessary, the definition of the building's load-bearing structure was based on reasonable assumptions regarding expected structural behavior and common construction practices of the time.

### **3.3 Materials**

The study, being limited to a comparative analysis of results obtained through different calculation methods, did not include any in-situ material testing.

As a result, the compressive strength of the concrete, the type of materials, and the exact arrangement of the reinforcement bars remain unknown.

In the absence of direct test results, the mechanical properties of concrete and reinforcing steel were defined based on previous studies that examined the evolution of material characteristics over time.

#### **3.3.1 Concrete**

The estimation of compressive strength of concrete in an existing reinforced concrete structure can be performed using the model proposed by Fantilli from Politecnico di Torino. This approach derives the strength parameter as a function of the construction year, utilizing strength-age curves (Fantilli and Ferraro, 2020).

Figure 6, based on 100 years of structural concrete certification data, illustrates the distribution of average cubic strength ( $R_c$ ) values, including the 5%, 25%, 75%, and 95% percentiles.

Given that the building under study was constructed beginning in 1961, with its design dating back to approximately 1956, it was assumed—based on the available data—that the in-situ concrete likely possesses mechanical characteristics comparable to those of modern C20/25 concrete.

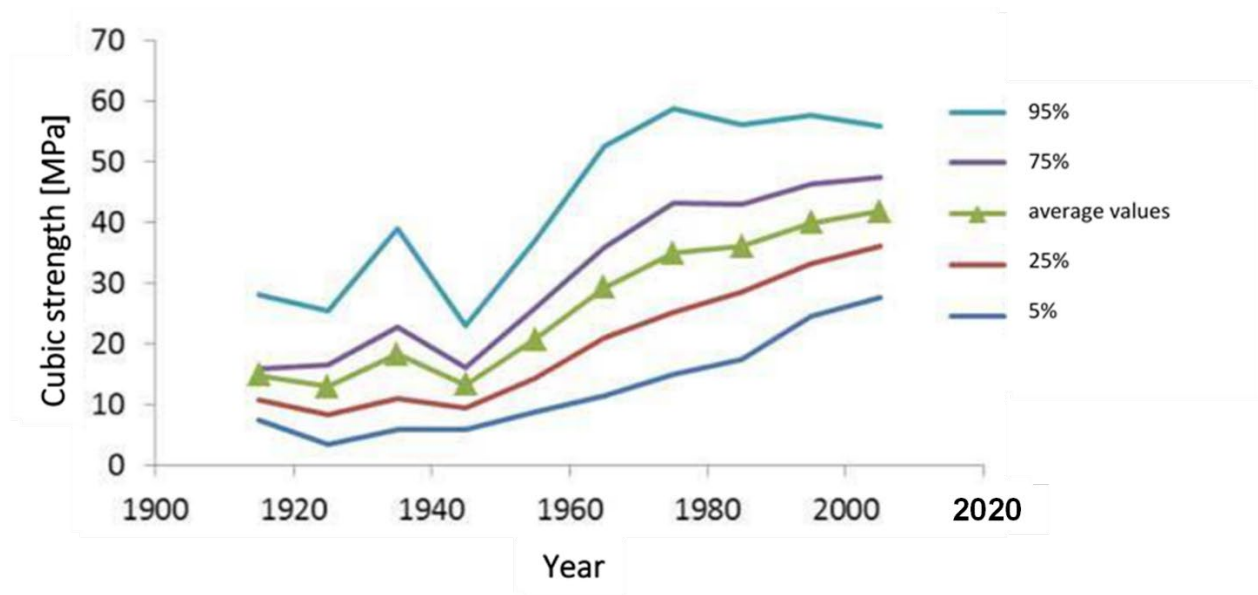


Fig. 6. Cubic strength of structural concrete as a function of year of construction. Taken from Fantilli, and Ferraro, 2020.

### 3.3.2 Steel

Similarly, to estimate the mechanical properties of the existing steel reinforcement, reference was made to a study conducted by the Department of Structural Engineering at the University of Naples "Federico II" (Fig. 7). This research presents a statistical analysis of the mechanical properties of reinforcement steel used in Italy between 1950 and 1980 (Verderame et al., 2011).

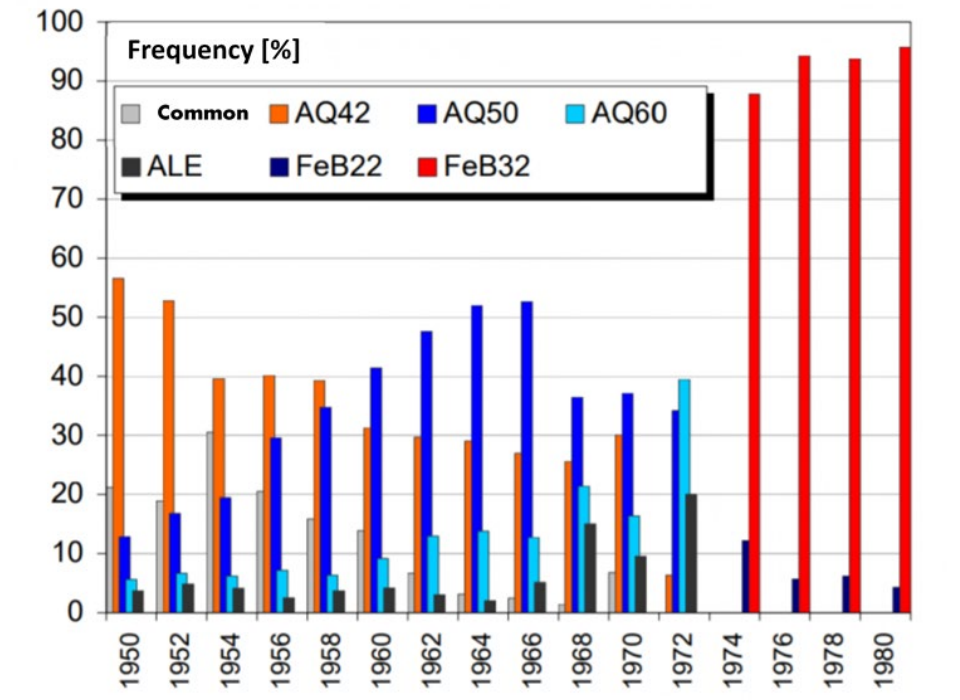


Fig. 7. Frequency distribution for various steel types as a function of year of construction. Taken from (Verderame et al., 2011).

#### 4. Objective of the analysis and working assumptions

The objective of the present analysis was to assess the effectiveness of a simplified schematic representation of the structure, as implemented in the TaBu software, for obtaining horizontal displacements induced by wind and/or seismic actions. The extensive computational capabilities of TaBu are described in Section 6.

This evaluation was conducted by comparing the results obtained from the simplified TaBu model with those derived from a detailed FEM model developed using the commercial software DOLMEN. Since the exact dimensions of certain structural elements (e.g., beams, columns, and shear walls) were partially unknown, plausible structural assumptions were made to define these geometrical parameters.

The structural analyses were not intended for building purposes but rather for evaluating the structural response under horizontal loading. Given the limited availability of detailed structural data, the assessment of stresses was performed only on wall W4, shown in Fig. 5, and reported in the Appendix.

On the other hand, the study focused on comparing the displacement obtained from the two different computational methodologies.

## 5. Modeling with TaBu: General Algorithm and Analytical Formulation

The TaBu (Tall Building Structural System) computational code, developed within the Matlab environment, is based on a robust analytical model known as the General Algorithm (GA). This code is designed to facilitate rapid data input and enable prompt evaluation of design modifications for high-rise structures. The core of the methodology is derived from the foundational work by Capurso (Capurso, 1981) and Carpinteri (Carpinteri and Carpinteri, 1985) and has been further developed in recent years (Carpinteri et al., 2010, 2013, 2014, 2016; Lacidogna, 2017; Nitti et al., 2021), to analyze a wide range of building typologies.

### 5.1. General Algorithm and Structural Discretization

The GA formulation models the entire building by connecting all vertical bracings (frames, cores, walls) at each floor level through infinitely rigid slabs in their own plane but infinitely deformable out-of-plane. Each vertical bracing is localized in its own local reference system (origin at the shear center, axes parallel to the principal inertia directions).

The model's computational efficiency stems from a drastic reduction in degrees of freedom (DOFs). For an  $N$ -story building, the model considers only three DOFs per floor, counted from top to bottom. The unknown displacement vector for each floor is  $\{\delta\} = \{\{\xi\}; \{\eta\}; \{\vartheta\}\}$ , representing the two translations (along the global  $x$  and  $y$  axes) and the rigid rotation around the  $z$ -axis.

### 5.2. Static Analysis Formulation

The external load vector applied to the structure is  $\{F\} = \{\{p_x\}; \{p_y\}; \{m_z\}\}$ , consisting of lateral forces and torsional moments at each floor.

The local stiffness matrix  $[\bar{K}_i]$  of each  $i$ -th bracing, defined in its local reference system, relates the internal loads it carries to the floor displacements:

$$\{F_i\} = [\bar{K}_i]\{\delta\}. \quad (1)$$

Global equilibrium is enforced by summing the contributions of all  $M$  bracings, leading to the global stiffness matrix  $[\bar{K}]$  of the entire building:

$$\{F\} = \sum_{i=1}^M \{F_i\} = (\sum_{i=1}^M [\bar{K}_i]) \{\delta\} = [\bar{K}] \{\delta\}. \quad (2)$$

The distribution of the external load  $\{F\}$  to each individual bracing is calculated using the distribution matrix  $[R_i]$ :

$$\{F_i\} = [\bar{K}_i][\bar{K}]^{-1}\{F\} = [R_i]\{F\}. \quad (3)$$

Once the forces on a bracing  $\{F_i\}$  are known, Eq. (1) can be inverted to determine the displacements  $\{\delta\}$  and, consequently, the internal stresses acting on that element.

### 5.3. Dynamic Analysis Formulation

For dynamic analysis, the building is modeled as an equivalent cantilever beam with floor masses concentrated at their centers of gravity. The undamped equation of motion is:

$$[M]\{\ddot{\delta}\} + [K]\{\delta\} = \{0\}, \quad (4)$$

where  $[M]$  is the mass matrix and  $[K]$  is the global stiffness matrix. Assuming the solution can be separated into a spatial component  $\{\zeta(z)\}$  and a temporal component  $\psi(t)$ , such that  $\{\delta\} = \{\zeta(z)\} \psi(t)$ , Eq. (4) leads to the eigenvalue problem:

$$\det([K] - \omega_n^2[M]) = 0. \quad (5)$$

Solving this yields  $3N$  eigenvalues ( $\omega_n$ ), from which the natural frequencies ( $f_n = \omega_n/2\pi$ ) and periods of vibration ( $T_n = 1/f_n$ ) are derived. The corresponding eigenvectors  $\{\zeta(z)\}$  represent the mode shapes of the building (Carpinteri, 2016; Nitti, 2021; Zalka, 2001).

### 5.4. Model Advantages and Limitations

This analytical approach provides detailed insights into stress distributions and dynamic characteristics while offering significant advantages:

- Drastically reduced computation times compared to commercial FEM software due to the low number of DOFs.
- No meshing is required.

- Simplified and rapid input process.

- Results generally align well with FEM analyses, typically exhibiting deviations of less than 10% (Carpinteri et al. 2013, 2014), which is acceptable for preliminary design phases. Fig. 8 illustrates the simplified model of the tower discretized using TaBu.

The model's efficiency imposes simplifications on the modeling process:

- Floors are assumed to be rectangular.

- Frames are modeled as independent planar elements with constant spans and constant member cross-sections.

- All elements are clamped at the base.

- Elements modeled with Vlasov's theory (Vlasov, 1961) for thin-walled sections have constant thickness.

This methodology provides a versatile and efficient conceptual tool for the initial 3D design of tall buildings, allowing for accurate modeling of lateral load distribution, secondary effects, and dynamic characteristics.

### AXONOMETRIC VIEW

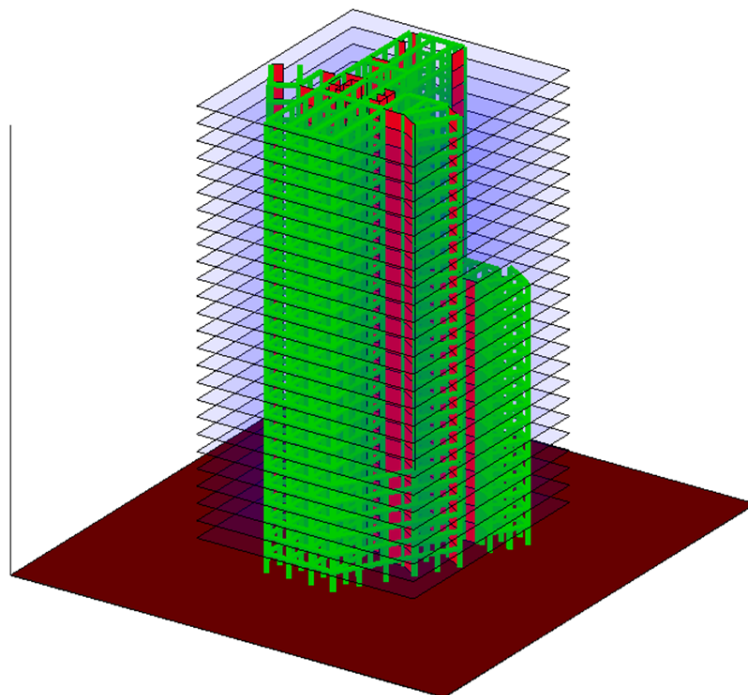


Fig. 8. Simplified model of the Livorno Tower discretized with TaBu.

## 6. Modeling with DOLMEN

Based on the floor plans identified in the literature and supported by several in situ measurements, a geometric representation of the building was obtained with a satisfactory degree of approximation.

Given the general geometry of the typical floors, the vertical load-bearing elements (columns and shear walls) were identified, and the arrangement of the main beams and slabs was assumed accordingly.

Using the five identified typical floor plans, structural schemes of the corresponding building levels were developed. The cross-sections of the individual structural elements (beams and columns), which were not entirely known, were defined based on plausible design assumptions.

For the floors without any graphical documentation, structural layouts were generated by analogy with the documented ones, considering the overall structure of the building.

Using the extensive structural modeling capabilities of DOLMEN, the complete structural model was successfully generated.

Obviously, the generation of the structural floor plans required certain approximations due to the lack of detailed information regarding the cross-sectional dimensions of structural elements.

The floor plans were vertically connected by inserting the corresponding column and wall elements maintaining a constant inter-story height of 3.20 meters, except for the ground floor, which is separated from the first floor by a height of 3.60 meters.

The FEM model generated in DOLMEN, assuming the use of concrete comparable to class C20/25, can be considered sufficiently representative of the real structure in terms of global geometry.

It is important to emphasize that the FEM scheme was not intended for a detailed assessment of structural elements but rather at evaluating the global behavior of a tall building typology. Consequently, the detailed assumptions regarding the dimensions of the structural elements

introduced in the calculations, being consistently applied in both the TaBu and FEM models, retain their validity and do not compromise the results of the comparison despite potential deviations from the actual dimensions.

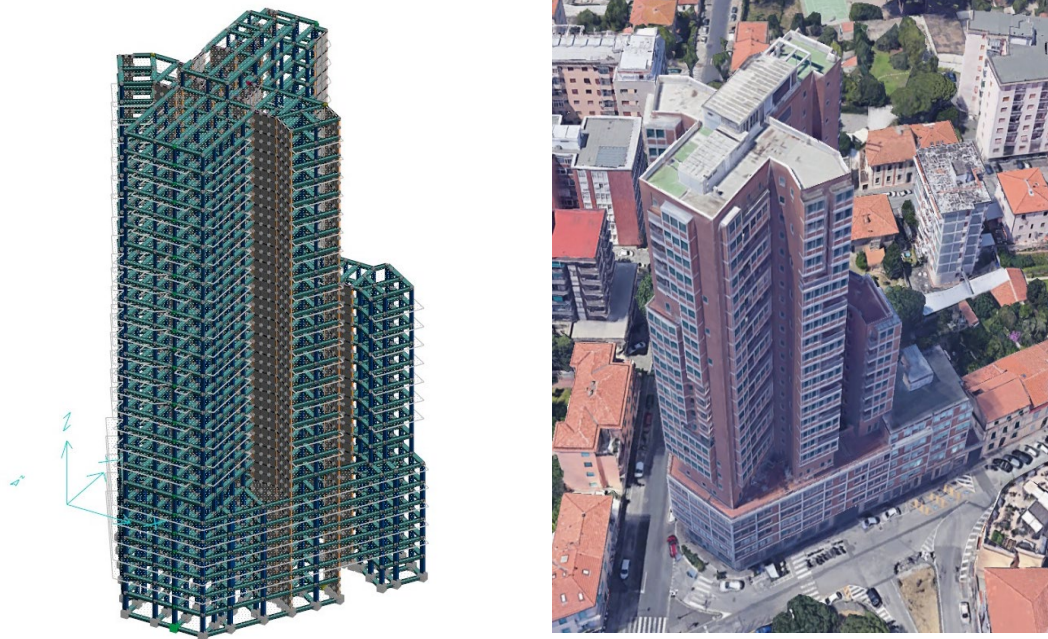


Fig. 9. FEM model made with CDM DOLMEN and view of the real structure.

The FEM model consists of the following elements (Fig. 9):

- 5693 one-dimensional beam elements;
- 3203 two-dimensional shell elements;
- 400 slabs;
- 5533 nodes.

In analogy to the simplified modeling approach adopted in TaBu, the assumption of infinitely rigid slabs within their own plane was also adopted in the FEM model.

The seismic forces were defined based on the parameters shown in Fig. 10.

Seismic Analysis Parameters (according to NTC 2018 “Nuove norme sismiche per il calcolo strutturale”, DM 17 January 2018):

- Building location = LIVORNO (long.  $10^{\circ}32'$ , lat.  $43^{\circ}55'$ )

- Ground type = C
- Stratigraphic Amplification Coefficient  $S_s = 1.500$
- Topographic Amplification Coefficient  $S_T = 1.000$
- S factor = 1.500
- Design life of the structure  $V_N = 50$  years
- Importance Factor  $C_U = 1.0$
- Reference Period  $V_R = 50.0$
- Behaviour Factor  $q = 1.500$

Dati generali per sismica (NTC 2018)

Zona | Suolo | Topografia | Fattore comport. q | Dati progetto | Vulnerabilità

Località: LIVORNO

Comune: Livorno (Livorno) - Toscana

Zona sism.: 3

Latitudine: 43.5501

Longitudine: 10.3209

Applica | Applica e chiudi | Chiudi

Dati generali per sismica (NTC 2018)

Zona | Suolo | Topografia | Fattore comport. q | Dati progetto | Vulnerabilità

A - Ammassi rocciosi affioranti o terreni molto rigidi  
 B - Rocce tenere e depositi di terreni a grana grossa o terreni a grana fina molto consistenti  
 C - Depositi di terreni a grana grossa mediamente addensati, o terreni a grana fine mediamente consistenti  
 D - Depositi di terreni a grana grossa scarsamente addensati o di terreni a grana fine scarsamente consistenti  
 E - Terreni dei sottosuoli di tipo C o D per spessore non superiore a 30 m

Applica | Applica e chiudi | Chiudi

Dati generali per sismica (NTC 2018)

Zona | Suolo | Topografia | Fattore comport. q | Dati progetto | Vulnerabilità

Coefficiente di amplificazione topografica: 1.00

Tab.3.2V - Valori massimi del coefficiente di amplificazione topografica

Categoria topografica	Ubicazione dell'opera o dell'intervento	$S_T$
T1	-	1,0
T2	In corrispondenza della sommità del pendio	1,2
T3	In corrispondenza della cresta del rilievo	1,2
T4	In corrispondenza della cresta del rilievo	1,4

Applica | Applica e chiudi | Chiudi

Dati generali per sismica (NTC 2018)

Zona | Suolo | Topografia | Fattore comport. q | Dati progetto | Vulnerabilità

Per azioni verticali:  
q: 1.50

Per azioni orizzontali:  
q: 1.50 | Assegnato

$q = q_0 \cdot K_R = 1.88 \cdot 0.80$

Classe di duttilità: Classe di duttilità "B" (bassa)

$q_0$ : 1.88

$K_R$ : 0.8 (Edifici non regolati in altezza)

Applica | Applica e chiudi | Chiudi

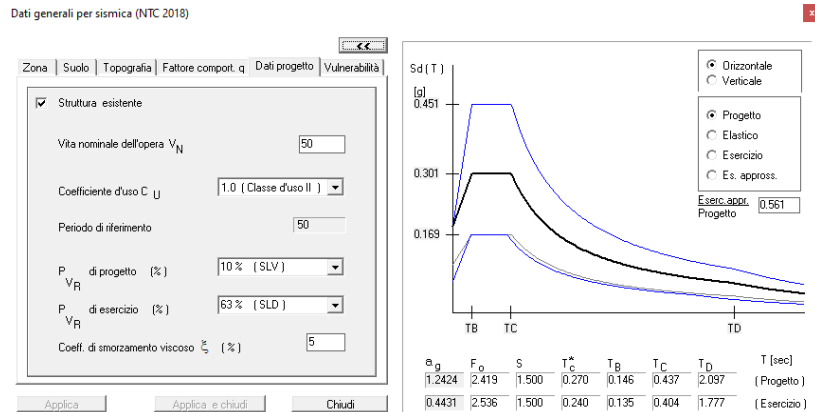


Fig. 10. Parameters adopted for the seismic actions on the Livorno Tower

## 7. Performed analyses

The analyses were conducted based on the adopted working hypotheses, with the primary objective of comparing the horizontal displacements estimated with the two methodologies (TaBu model and FEM). These comparisons were carried out under the following four loading conditions:

- Wind action in the X direction;
- Wind action in the Y direction;
- Seismic action in the X direction;
- Seismic action in the Y direction.

Two structural models were developed: the analytical model through the TaBu software and the finite element model (FEM) created with CDM DOLMEN software.

The detailed discretization of the structure enabled by DOLMEN necessitated appropriate refinements to facilitate a meaningful comparison with the results obtained using TaBu.

As a preliminary step, an operational calibration phase was undertaken to ensure adequate consistency between the two models. This phase involved testing simplified models to properly represent the assumptions inherent to TaBu, particularly regarding floors, which are considered infinitely rigid within their plane and infinitely deformable outside it. Additionally, this phase aimed to optimally define the constraints between structural elements.

The comparison of the results obtained from both models under the four loading conditions was intended to assess the degree of correspondence between the two approaches.

## 8. Comparison between analytical model and FEM

The FEM model developed with DOLMEN was employed to estimate horizontal displacements (in both the X and Y directions) and the rotation at a point near the barycenter of each floor (Fig. 11).

After the identification of the nodes of each floor corresponding to the desired geometric location, the data export functionalities provided by DOLMEN (Fig. 12) were utilized to generate simple tables containing the required displacements and rotations. The export of data in a format compatible with Excel enabled an efficient and rapid graphical interpretation.

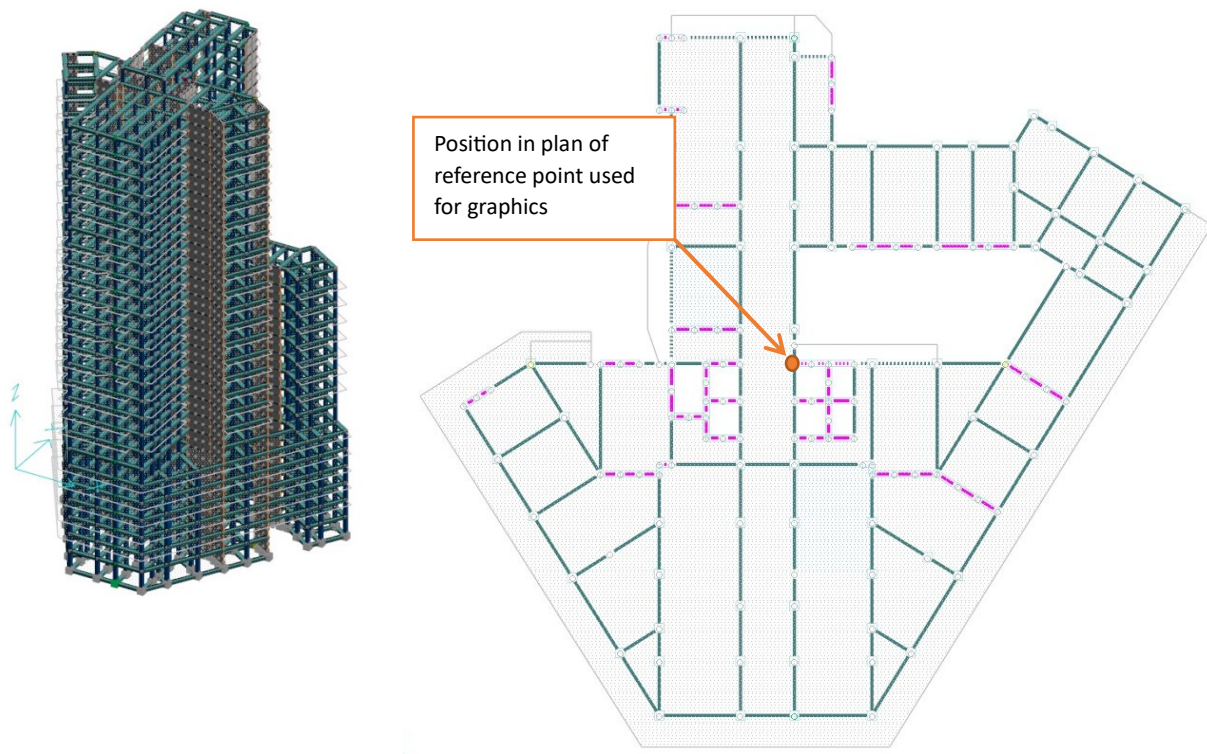


Fig.11. FEM model developed with CDM DOLMEN and chosen position for displacement measurements.

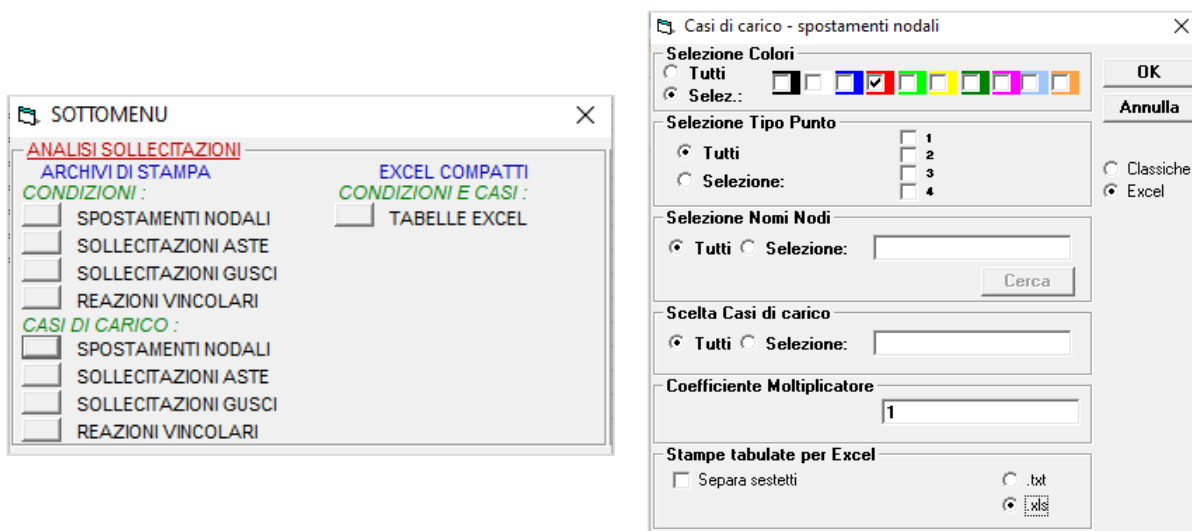


Fig.12. DOLMEN menu for reading and saving node displacement data (selected by color)

The same displacements and rotations were estimated using TaBu and subsequently compared with those obtained from DOLMEN.

Below, a comparative analysis of the results provided by the two software tools is presented.

The graphs illustrate horizontal displacements (X and Y) and rotations, where the results from DOLMEN are represented by the blue curve and those from TaBu by the red curve. In each graph, the horizontal axis represents the displacements or rotations, whereas the vertical axis corresponds to the floor levels.

A strong quantitative agreement is observed for both displacements and rotations due to wind action in the X and Y directions (Figs.13-15), as well as for displacements and rotations related to seismic action (Figs. 16 and 17).

For wind action in the X direction, the overall trends of the diagrams exhibit a high degree of similarity. The deviations between the values obtained for each floor using the two models are quantified as follows: in the direction of the applied load, the maximum deviation occurs at the top floor, reaching 22.61%; whereas in both the directions orthogonal to the load and in the case of the rotations, the greatest discrepancy is observed at the 15th floor, with a maximum deviation of 31.68% and 30.99%, respectively.

### Wind action in the X direction

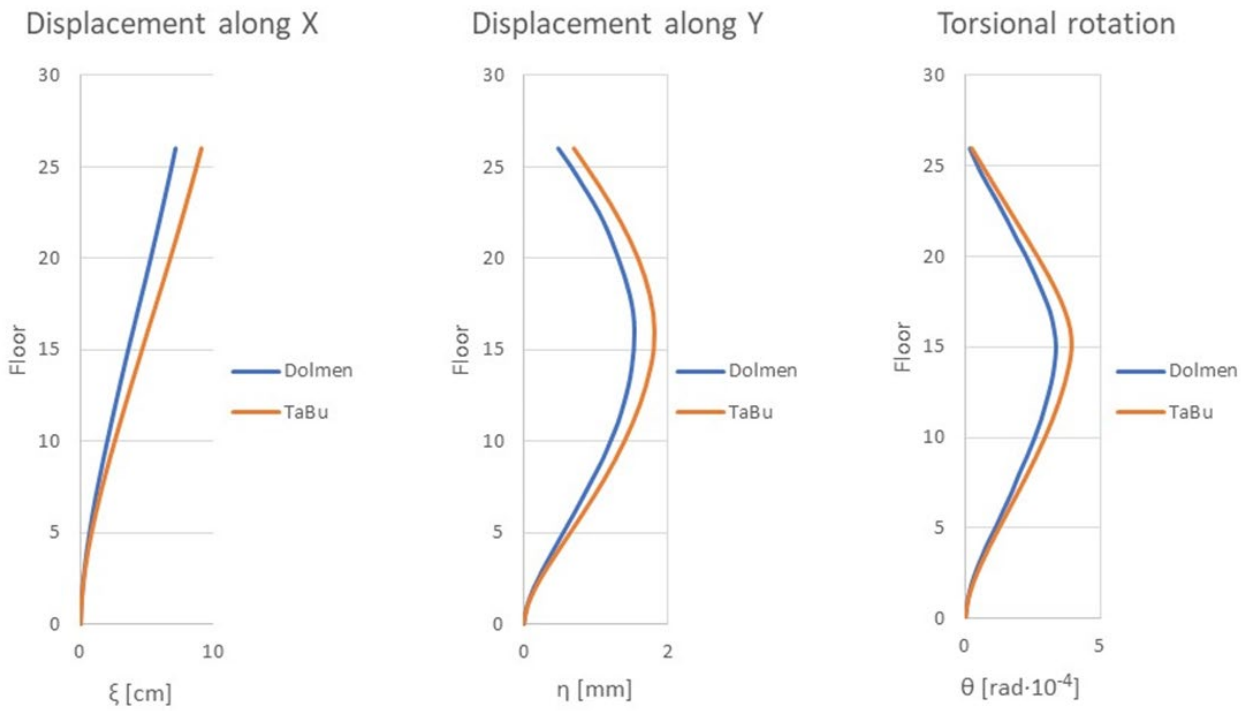


Fig. 13. Comparisons of displacements and rotations due to wind action acting in the X direction obtained with the FEM model developed with DOLMEN and the TaBu code.

### Wind action in the X direction

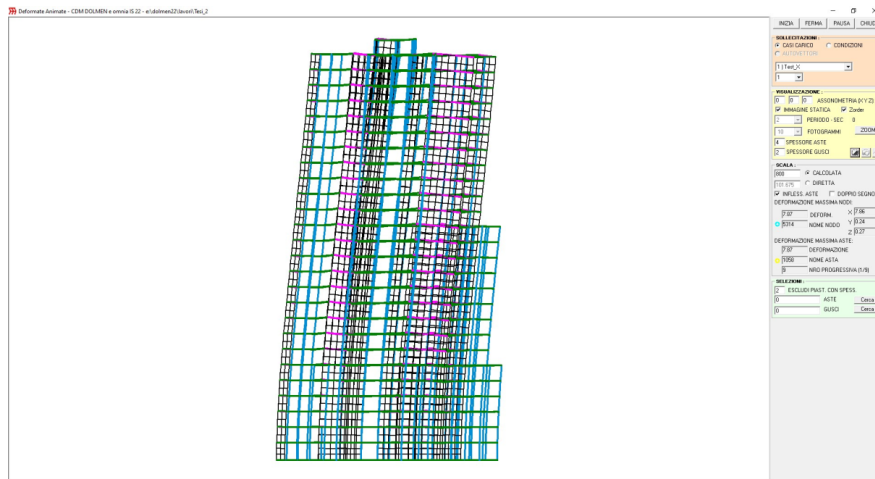


Fig. 14. Deformed shape for displacements along the X-axis due to wind action in the X direction obtained from the FEM model developed with DOLMEN

For wind action in the Y direction, the smallest deviation between the diagrams is again recorded in the direction of the applied load, with a maximum deviation of 19.59% at the top floor. The maximum deviation in the orthogonal direction to the applied load is also recorded at the top floor, reaching 32.42%. For rotations, the maximum discrepancy is again observed at the top floor, amounting to 29.27%.

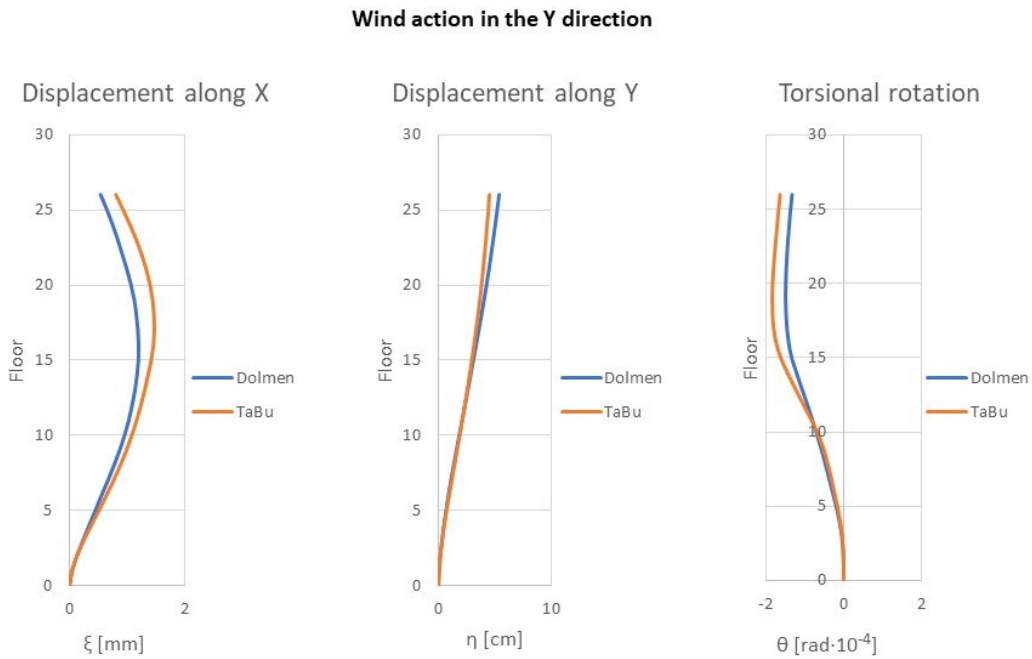


Fig. 15. Comparisons between displacements and rotations induced by wind action in the Y direction, obtained using the FEM model developed with DOLMEN and the TaBu code.

Finally, considering the seismic action in the Y direction (Figs. 16 and 17), the following differences between the FEM model developed with DOLMEN and the TaBu code were observed: in the Y direction (direction of the applied load), the maximum deviation in displacements occurs at the top floor, reaching 23.51%; in the orthogonal X direction, a maximum deviation of 17.56% is observed at the same level. For rotations, the diagrams are nearly superimposed, with a maximum deviation of 18.97%, again measured at the top floor.

## Primary seismic load acting in the Y direction

Load acting in Y direction

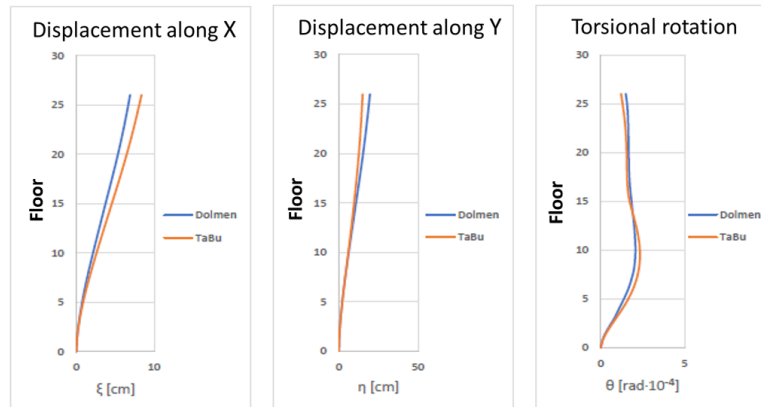


Fig. 16. Comparisons between displacements and rotations induced by seismic action in the Y direction, obtained using the FEM model developed with DOLMEN and the TaBu code.

## Primary seismic load acting in the Y direction

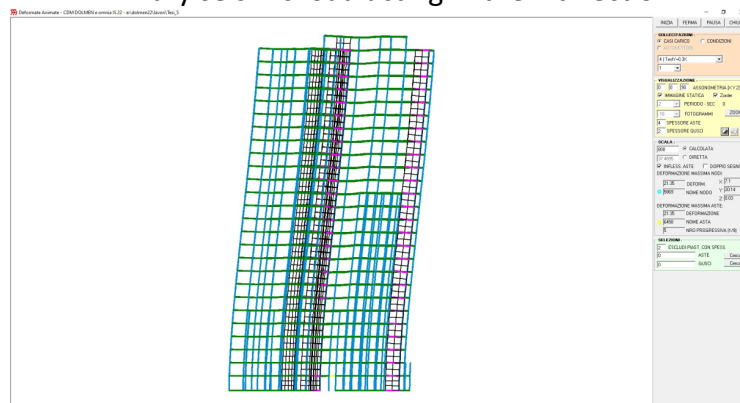


Fig. 17. Deformed shape for displacements along the Y-axis due to seismic action in the X direction obtained from the FEM model developed with DOLMEN.

It is worth noting that the discrepancies between 20 and 30% observed when comparing the results of the analytical model with those of the FEM model is primarily due to the complex and unconventional architecture of the Michelucci Tower, which challenges the simplifications inherent in the analytical approach. While some data assumptions are involved in both models, the idealized analytical model assumes regular, rectangular floors and uniform structural elements (Carpinteri et

al., 2013, 2014). These simplifications lead to less accurate results, especially given the tower's intricate geometry, featuring projections, bow windows, and irregular load paths.

When structural continuity, especially along the vertical development, is interrupted—as in this case—local effects captured by the detailed FEM model may not be perfectly simulated by the analytical approach. Nonetheless, despite these differences, the analytical model effectively captures the irregular and non-trivial behaviors of displacements and torsional rotations, as shown in the graphs of Figures 13, 15, and 16, which are derived from the FEM model.

## 9. Conclusions

The Michelucci Tower in Livorno, a remarkable example of Italian architectural and construction capabilities from the early 1960s, was conceived by the inventive genius of Giovanni Michelucci, one of the most renowned Italian architects of the 20th century, was chosen as the reference structure for comparing the results of two distinct computational approaches on tall buildings. The first approach, characterized by a more schematic and expedite analytic computation of the structure, was implemented through the TaBu software, which offers a simplified modeling process and greater computational efficiency in estimating horizontal displacements due to wind and seismic actions. The second approach, involving a more detailed representation of the geometry, loading conditions, and mechanical behavior of the structure, was conducted through the development of a three-dimensional FEM model using the DOLMEN software.

The comparison between the results from the two software programs, focusing on the horizontal displacements induced by wind and seismic loads, demonstrate a reasonable level of agreement, with maximum deviations ranging from 20% to 30%. However, it is essential to emphasize that one of the main advantages of using the TaBu software lies in its extraordinary computational speed. It is indeed believed that the ratio between the processing times required by a FEM analysis, which has six degrees of freedom per node, and those needed for TaBu, which has three degrees of freedom per floor, is proportional to the square of the ratio between the number of degrees of freedom of the two

systems. This means that, as the complexity of the structure increases, TaBu can ensure a significant saving in time, making it a particularly efficient tool for preliminary structural analysis.

Given the relatively modest discrepancies in horizontal displacement estimates between the two models, it is recommended that rapid and simplified preliminary analyses using TaBu be conducted during the early design stages of tall buildings. These initial assessments can provide valuable guidance for early design decisions, which should subsequently be validated through more refined FEM models to ensure greater accuracy and reliability.

### **Appendix: Stresses comparison in wall W4**

Following the displacement analysis, another important application in structural calculation involves the stresses acting on the bracing cores. It is important to clarify that Dolmen software cannot provide point-specific values at the vertices of the two-dimensional shell elements. Instead, it gives values at the centroids of the triangles that make up each shell element.

Therefore, for a given load case, the comparison was made between the TaBu model and the FEM model using the average values calculated at the base of wall W4 (see Fig. 5), which is the most stressed wall. The term “average” refers to the mean of the values calculated analytically at two vertices and at the midpoint of a section segment in the TaBu model.

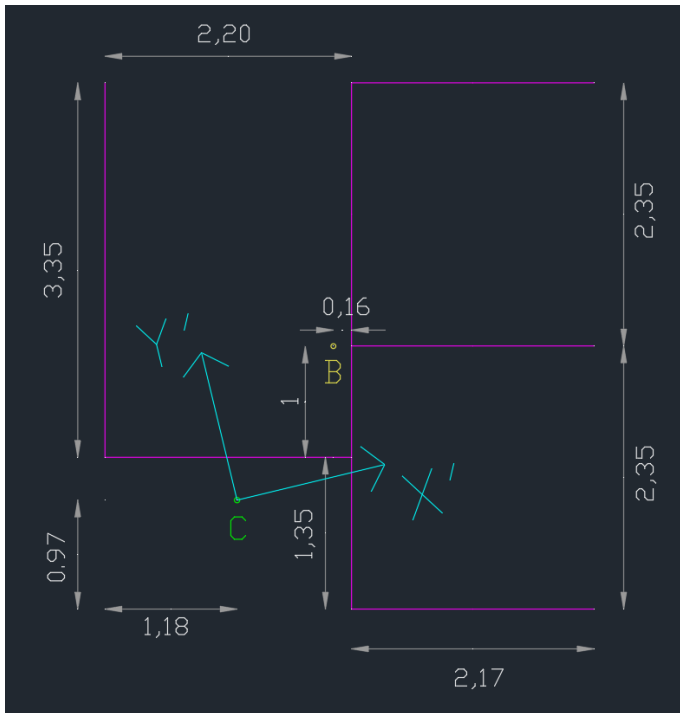
As an example, the plan of a representative bracing element subjected to wind loads in the X-direction is shown in Fig. 1A. The type of shear wall section is a Vlasov thin open section.

In building studies, Vlasov-type sections are generally of greater interest because, due to their more varied configurations, they can sometimes be the only types present. The Michelucci Tower includes several vertical elements with Vlasov sections, but the most notable one is called W4 (see Fig. 5).

#### **Stress calculation procedure**

Starting from the applied loadings and geometric properties entered into the TaBu software, the stresses acting on various sections of the bracing wall were calculated. Unlike the displacement results, which are provided directly by the software, these stresses require a detailed analysis.

Therefore, the illustration of the section is shown in Fig. 1A to extract the necessary information for this calculation. All data related to the section, including the coordinates of the centroid, the center of shear, moments of inertia, etc., are also presented in the table of Fig. 1A.



<b>Thickness</b>	
<b>b</b>	0.4 m
<b>Centroid coordinates</b>	
<b>X<sub>g</sub></b>	-6.64 m
<b>Y<sub>g</sub></b>	-2.42 m
<b>Shear center coordinates</b>	
<b>X<sub>c</sub></b>	-7.5 m
<b>Y<sub>c</sub></b>	-3.8 m
<b>Moments of inertia</b>	
<b>J<sub>xx</sub></b>	16.04 m <sup>4</sup>
<b>J<sub>yy</sub></b>	11.57 m <sup>4</sup>
<b>J<sub>ωω</sub></b>	15.56 m <sup>6</sup>
<b>J<sub>xy</sub></b>	0 m <sup>4</sup>
<b>J<sub>xω</sub></b>	0 m <sup>5</sup>
<b>J<sub>yω</sub></b>	0 m <sup>5</sup>
<b>Torsional stiffness factor</b>	
<b>J<sub>t</sub></b>	0.3575467 m <sup>4</sup>
<b>Principal axes rotation angle</b>	
<b>Omega ω</b>	13.56 °

Figure 1A: Schematic section of wall W4. All relevant data, including the coordinates of the centroid, the shear center, moments of inertia, etc., are summarized in the table accompanying the figure.

### Geometrical coordinate system and stress calculation

Given that, as indicated in Section 5.1, each vertical bracing element is located in its own reference system (origin at the shear center, axes parallel to the principal axes of inertia), and for this reason all mixed moments of inertia are null, the stresses are then calculated at nine points in the vertices of the section using the following equations.

#### Normal stresses

$$\sigma_z = \frac{M_x}{J_{xx}} y + \frac{M_y}{J_{yy}} x + \frac{B}{J_{\omega\omega}} \omega, \quad (1A)$$

where the terms  $M_x$ ,  $M_y$ , and the bimoment,  $B$ , are known from the software.

#### Shear stresses

Shear stresses following Vlasov theory acting along the cross-section:

$$\tau_{(s)} = \frac{T_x S_y}{J_{yy} b} + \frac{T_y S_x}{J_{xx} b} + \frac{M_z^{VL} S_\omega}{J_{\omega\omega} b}, \quad (2A)$$

where the terms  $T_x$ ,  $T_y$ , and the Vlasov moment,  $M_z^{VL}$ , are known from the software.

Shear stresses following De Saint Venant theory acting along the cross-section:

$$\tau_{(s,T)} = \frac{M_z^{SV}}{J_t} b. \quad (3A)$$

In the previous equations, the static moments  $S_y$ ,  $S_x$ , and  $S_\omega$ , must also be calculated analytically. For sake of simplicity the calculations of their values are omitted here; for further details, see Carpinteri et al. 2010.

The stress characteristics at the base of the wall W4, due to wind loads acting in the X-direction, are reported in the following table:

$M_x$ [kNm]	-11037.17
$M_y$ [kNm]	28612.86
$B$ [kNm <sup>2</sup> ]	-753.97
$T_x$ [kN]	1392.74
$T_y$ [kN]	-563.32
$M_{z,VL}$ [kNm]	93.41
$M_{z,SV}$ [kNm]	0.00

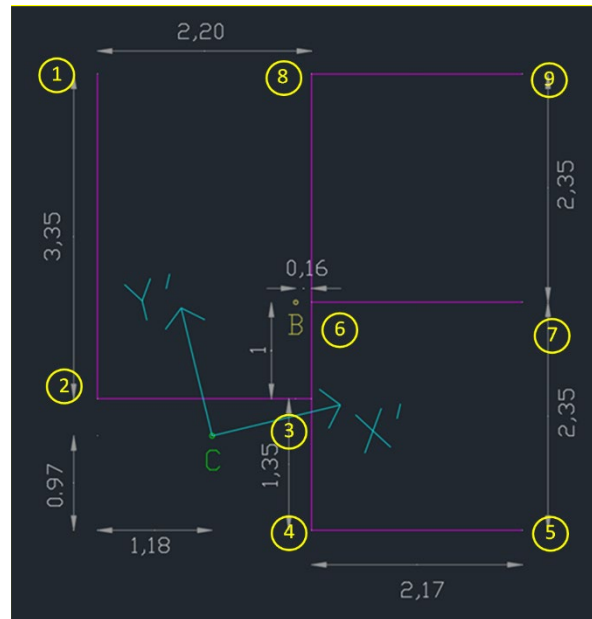


Fig. 2A. Numbering of the edges of the shear wall W4.

Then, referring to Fig. 2A, which shows the numbering of the section edges, the normal stresses at the base of the wall W4 are determined:

Point	$\sigma_{M_x}$ [KN/m <sup>2</sup> ]	$\sigma_{M_y}$ [KN/m <sup>2</sup> ]	$\sigma_B$ [KN/m <sup>2</sup> ]	$\sigma$ [KN/m <sup>2</sup> ]
1	-1617.04	-5044.96	147.79	-6514.22
2	688.10	-5044.96	-43.61	-4400.47
3	688.10	395.68	-3.39	1080.39
4	1617.04	395.68	63.96	2076.69
5	1617.04	5762.14	-39.25	7339.93
6	0.00	395.68	-52.33	343.35
7	0.00	5762.14	91.58	5853.72
8	-1617.04	395.68	-168.62	-1389.98
9	-1617.04	5762.14	222.41	4367.51

While, the following values are obtained for the Vlasov shear stresses:

Point	$\tau_{T_x}$ [kN/m <sup>2</sup> ]	$\tau_{T_y}$ [kN/m <sup>2</sup> ]	$\tau_{M_z}$ [kN/m <sup>2</sup> ]	$\tau$ [kN/m <sup>2</sup> ]
1	0.00	0.00	0.00	0.00
2	821.56	79.02	21.61	922.19
3 → 2	1068.33	1.76	15.01	1085.09
3 → 4	-352.10	-258.13	8.25	-601.97
3 → 6	-716.23	256.37	-23.26	-483.12
4	-325.01	-179.11	3.30	-500.82
5	0.00	0.00	0.00	0.00
6 → 3	701.19	-274.81	19.96	446.34
6 → 7	-325.01	0.00	5.10	-319.91
6 → 8	-376.17	274.81	-25.06	-126.43
7	0.00	0.00	0.00	0.00
8	-325.01	179.11	7.20	-138.70
9	0.00	0.00	0.00	0.00

Regarding the shear stresses according to De Saint Venant's theory, since the torsional rotation of the wall is zero at the base, the torsional moment is also zero. Therefore, at each point at the base, we have:

$$\tau_{(s,T)} = 0 \frac{\text{kN}}{\text{m}^2}.$$

Considering the normal stresses and noting that the wall analyzed is the one between vertices 1 and 2 (see Fig. 2A), the results obtained from the FEM model graphical output, generated using Dolmen software, are shown in Fig. 3A.



Fig. 3A. Section at the base of the wall depicted in the Dolmen, bounded by vertices 1 and 2, subjected to wind load acting along the X direction, with normal stresses in [daN/cm<sup>2</sup>].

Considering the shear stresses, the results obtained between vertices 2 and 3 from the FEM model in the Dolmen software are represented in Fig. 4A.



Fig. 4A. Section at the base of the wall depicted in the Dolmen, bounded by vertices 2 e 3, subjected to wind load acting along the X direction, with shear stresses in [daN/cm<sup>2</sup>].

### Comparison between the average values obtained from the FEM model and the analytical model

By converting all the values obtained in Dolmen to kN/m<sup>2</sup>, it is possible to proceed with the analytical method to calculate the average stress values between the endpoints of side 1-2 and the midpoint, as well as between the endpoints of side 2-3 and the midpoint. These values are based on the data listed

in the previous tables. From the comparison, it is evident that the overall differences between the average stresses computed from the two models at the base of wall W4 are approximately 9.66% for the longitudinal stresses and 4.78% for the shear stresses.

## **Acknowledgements**

The authors would like to express their sincere gratitude to the Giovanni Michelucci Foundation for granting permission to utilize the archive sources of "Grattacielo Roma, Livorno 1956-1966" (<http://db.michelucci.it/archivi/progetti/?opera=P125>).

They also extend their heartfelt thanks to CDM DOLMEN - SOFTWARE DI CALCOLO STRUTTURALE (<https://cdmdolmen.it/>) for their valuable contribution to the structural calculations presented in this study.

Finally, the authors are deeply grateful for the sponsorship and financial support provided by Politecnico di Torino, Italy, which made this work possible through basic research funds.

## **References**

Capurso, M. (1981) Sul calcolo dei sistemi spaziali di controventamento, parte 1. *Giornale del Genio Civile*, 1-2-3, pp. 27–42.

Carpinteri, A. and Carpinteri, AN. (1985). Lateral loading distribution between the elements of a three-dimensional civil structure. *Computers and Structures*, 21(3), pp. 563–580.

Carpinteri, A., Lacidogna, G. and Puzzi, S. (2010). A global approach for three-dimensional analysis of tall buildings. *Structural Design of Tall and Special Buildings*, 19(5), pp. 518–536.

Carpinteri, A., Lacidogna, G. and Cammarano, S. (2013) Structural analysis of high-rise buildings under horizontal loads: A study on the Intesa Sanpaolo Tower in Turin. *Engineering Structures*, 56, pp. 1362–1371.

Carpinteri, A., Lacidogna, G. and Cammarano, S. (2014). Conceptual design of tall and unconventionally shaped structures: A handy analytical method. *Advances in Structural Engineering*, 17(5), pp. 767–783.

Carpinteri, A., Lacidogna, G. and Nitti, G. (2016). Open and closed shear-walls in high-rise structural systems: Static and dynamic analysis. *Curved and Layered Structures*, 3, pp. 154–171.

Fabbrizi, F. (2016). The variable city and its icon. The Livorno skyscraper by Giovanni Michelucci. *Firenze Architettura*, pp. 88–93.

Fantilli, A. and Ferraro, E. (2020). The strength of concrete cast in the first half of the 20th century. *Ingenio*. Available at: <https://www.ingenio-web.it/articoli/la-resistenza-dei-calcestruzzi-confezionati-nella-prima-meta-del-900/>

Lacidogna, G. (2017). Tall buildings: secondary effects on the structural behaviour. *Proceedings of the Institution of Civil Engineers – Structures and Buildings*, 170(6), pp. 391–405.

Luseroni, F. (2010). Giovanni Michelucci and the vertical city: the Livorno skyscraper. ETS Editions.

Nitti, G., Lacidogna, G. and Carpinteri, A. (2021). An analytical formulation to evaluate natural frequencies and mode shapes of high-rise buildings. *Curved and Layered Structures*, 8(1), pp. 307–318.

Verderame, G.M., Ricci, P., Esposito, M. and Sansiviero, F.C. (2011). Mechanical properties of steels used in reinforced concrete structures built from 1950 to 1980. In: *Proceedings of the 26th National AICAP Conference*; 19–21 May 2011; Padova, Italy.

Vlasov, V.Z., 1961. *Thin Walled Elastic Beams*. National Science Foundation, Washington, D.C.

Zalka, K.A. (2001) A simplified method for calculation of the natural frequencies of wall–frame buildings. *Engineering Structures*, 23, pp. 1544–1555.